Interpretation of in-plane and out-of-plane anisotropic surface–interface reflectance and transmittance difference spectroscopy

Tat-Kun Kwok, K. C. Tam, and Paul K. Chu

Department of Physics and Materials Science, City University of Hong Kong, Tat Chee Avenue, Kowloon, Hong Kong, China

Received March 17, 1997; revised manuscript received August 5, 1997

A numerical method developed previously [J. Appl. Phys. 80, 4621 (1996)] has been extended to simulate the nonnormal-incidence reflectance-difference spectroscopy and transmittance-difference spectroscopy spectra of biaxial anisotropic ($\epsilon_x \neq \epsilon_y \neq \epsilon_z$) multilayer systems with finite thickness. It is demonstrated that, when the principal axes of the anisotropy layer are at certain orientations, a reflectance-difference spectrum can be separated into two spectra, namely, an in-plane anisotropic spectrum and an out-of-plane anisotropic spectrum. It is shown that the separation is valid for large in-plane anisotropy, i.e., $|\epsilon_x - \epsilon_y| \approx |\epsilon_x|$, and an incident angle of $\leq 20°$. © 1998 Optical Society of America [S0740-3224(98)01203-X]

OCIS codes: 120.5700, 120.7000, 300.0300.

1. INTRODUCTION

Reflectance-difference (anisotropy) spectroscopy (RDS) is one of the few optical techniques that one can use to investigate the surfaces and the interface of semiconductor materials under steady-state conditions.[1-3] RDS spectra have been used successfully to measure various kinds of semiconductor layered structure, such as ZnSe/GaAs interfaces, atomic-layer epitaxy–grown ZnSe, Si–SiO_2 interfaces, (001) GaAs, III–V materials, and $Ga_{0.5}In_{0.5}P$.[4-10] The growth methods consist of molecular-beam epitaxy, atomic-layer epitaxy, organometallic vapor-phase epitaxy, ultrahigh-vacuum molecular-beam epitaxy, and metal-organic chemical-vapor deposition, among others.[4-10] RDS measures the optical anisotropy that is due to the difference between the incidence reflectance of light polarized along the two principal axes in the surface plane as a function of photon energy, thus providing information about electronic structure.

Transmittance-difference spectroscopy (TDS) is another optical technique that can probe the interface between a surface and a bulk substrate and is especially useful in investigation of transparent polymers. TDS is analogous to RDS, but instead of measuring the reflectance of polarized light it measures the transmittance of polarized light. TDS can truly elucidate the difference between s and p-polarized light at normal incidence. After optical measurements, e.g., RDS and TDS, that are functions of some physical parameters in which we are interested are obtained, a model must be developed that will permit us to predict accurately what should be measured from a sample of known properties.

The published analytical formalism used in modeling theoretical RDS spectra is based on two assumptions: The RDS spectra are measured at normal incidence and the thickness of the anisotropic interface d is much less than λ, the wavelength of the incident light.[6,11-13] The analytical formalism was summarized by Hingerl *et al.*[11,12] They considered a biaxial overlayer of thickness $d \ll \lambda$ whose principal dielectric tensor components in the crystal-coordinate system were ϵ_{xx}, ϵ_{yy}, and ϵ_{zz}. Here λ is the vacuum wavelength of light. They assumed that the dielectric functions of the ambient and isotropic substrate were ϵ_a and ϵ_s, respectively, where ϵ_a was real. Their analysis was based on Berreman's 4×4 matrix formalism.

Berreman's formalism states that the connection between input and output sides of the nth layer can be written as

$$\Psi_n = P_n \Psi_{n-1}, \tag{1}$$

where P is often called a propagator:

$$P = \exp[i(\omega/c)\mathbf{D}d]. \tag{2}$$

The solution of Eq. (1) is

$$\frac{\partial}{\partial z}\Psi = i\frac{\omega}{c}\mathbf{D}\Psi, \tag{3}$$

where D is the wave transfer matrix of rank 4 with components that depend on the principal dielectric tensor of the layer and the angle of incidence. Hingerl *et al.*[11,12] assumed that, for $d \ll \lambda$, one can evaluate the exponential of the propagator matrix by taking the first-order term, i.e.,

$$\exp[i(\omega d/c)\mathbf{D}] \cong \mathbf{I} + i(\omega d/c)\mathbf{D}, \tag{4}$$

where I denotes the 4×4 unity tensor. Finally, they arrived at the equation for normal-incidence RDS, i.e.,

$$\frac{\Delta r}{r} = \frac{4\pi i d n_a(\epsilon_{xx} - \epsilon_{yy})}{\lambda(\epsilon_s - \epsilon_a)}, \tag{5}$$

where $n_a^2 = \epsilon_a$.

0740-3224/98/031198-07$15.00

Yasuda *et al.* have developed an analytical method to correct interface RDS spectra for the relatively large effects of overlayer thickness.[6] They assumed a three-phase model consisting of a substrate s, an overlayer o of thickness d, and an ambient a. In this model the complex reflectance r is given by the Airy formula as

$$r = \frac{Zr_{so} + r_{oa}}{1 + Zr_{so}r_{oa}}, \tag{6}$$

where $Z = \exp(2ik_o d)$, $ck_o/\omega = n_o$ is the refractive index of the overlayer, c and ω are the velocity and the angular frequency of light, respectively, and r_{so} and r_{oa} are the complex normal-incidence reflectances at the substrate–overlayer and the overlayer–ambient boundaries, respectively. They assumed that the reflectance-difference (RD) spectrum arises from an anisotropy in r_{so} that is described by the small quantity Δr_{so}. They showed that

$$\left(\frac{\Delta r}{r}\right)_o = \frac{\left(\frac{\Delta r}{r}\right)_d (r_{so}r_{oa} + Z^{-1})(Zr_{so} + r_{oa})}{(r_{so}r_{oa} + 1)(r_{so} + r_{oa})}, \tag{7}$$

where $(\Delta r/r)_d$ is the anisotropy RD calculated for an overlayer of thickness d and $(\Delta r/r)_o$ is the anisotropy RD calculated for $d = 0$, i.e., without the overlayer.

The normal-incidence assumption made by Hingerl *et al.* and Yasuda *et al.* is inadequate because their RD spectra were acquired at near-normal incidence. Hingerl *et al.* and Yasuda *et al.* also assumed a thin interface layer. It is dangerous to assume a thin interface at a low-wavelength region comparable with the thickness of the interface. To obtain an accurate simulation of a three-phase layered structure, one should consider the interference of transmitted and reflected light beams formed inside the interface layer.

Kwok and Yang[15] have developed a numerical method based on the 2×2 matrices established by Yeh[14] to simulate the nonnormal-incidence RDS spectra of biaxial anisotropic ($\varepsilon_x \neq \varepsilon_y \neq \varepsilon_z$) multilayer systems. From the model it has been demonstrated that in the cases of near-normal incidence ($\simeq 5°$) and when the anisotropy within the layer plane (in-plane anisotropy) is small ($\varepsilon_x - \varepsilon_y \ll \varepsilon_x$) a RDS spectrum can be separated into two spectra, namely, an in-plane anisotropic spectrum and an out of-plane anisotropic spectrum.[16]

In this paper we extend the discussion, for the first time to our knowledge, to include the simulation of TDS. We demonstrate numerically that when the principal axes of the anisotropy layer are at certain orientations, a RDS or a TDS spectrum can be separated into two spectra, namely, a biaxial spectrum that is produced by the in-plane anisotropy ($\varepsilon_x \neq \varepsilon_y$) and a uniaxial spectrum that is produced by the out-of-plane anisotropy ($\varepsilon_x \neq \varepsilon_z$, $\varepsilon_y \neq \varepsilon_z$). We show that the separation is valid for large in-plane anisotropy, i.e., that $|\varepsilon_x - \varepsilon_y|$ is comparable with $|\varepsilon_x|$, and that the incident angle is $\leqslant 20°$. The numerical method can systematically handle more-complicated layered structures when necessary.

2. FORMALISM

Previously Kwok and Yang considered a layered structure consisting of a substrate followed by an interface, an overlayer, and an ambient.[15] It was assumed that the substrate was too thick for the light beam to pass through it, i.e., that there was no transmitted light.[15] Here we assume a layered structure consisting of a substrate s, an interface i of thickness d_i, an overlayer o of thickness d_o, a front ambient fa, and a back ambient ba. A light beam polarized at 45° to the incident plane with incident angle θ_a will be partially reflected and partially transmitted among the overlayer, the interface, and the substrate many times. It can be seen that the reflectance of the light beam is different from that in the previous case,[15] and three more matrices must be included in the formulas. We summarize the formulas and emphasize the effect of the incidence angle as follows.

Again we can resolve the incident polarized beam into two components, s (the electric field vector is parallel to the surface) and p (the electric field vector is perpendicular to the surface and the beam path). Suppose that the materials of the substrate, the interface overlayer, and the ambient are isotropic and homogeneous; then the s and the p waves will propagate along the same path. According to Yeh,[14] the amplitudes of the incident beam A_a, the reflected beam B_a, and the transmitted beam A_s can be calculated by 2×2 matrix multiplication as

$$\begin{bmatrix} A_{fa} \\ B_{fa} \end{bmatrix} = D_{fa}^{-1} D_o P_o D_o^{-1} D_i P_i D_i^{-1} D_s P_s D_s^{-1} D_{ba} \begin{bmatrix} A_{ba} \\ B_{ba} \end{bmatrix}. \tag{8}$$

$B_{ba} = 0$ because the light beam will not be reflected back to the substrate from the back ambient. P_o, P_i, and P_s are the propagation matrices in the form

$$P_\alpha = \begin{bmatrix} \exp(i\varphi_\alpha) & 0 \\ 0 & \exp(-i\varphi_\alpha) \end{bmatrix}, \tag{9}$$

where $\varphi_\alpha = 2\pi d_\alpha \cos\theta_\alpha n_\alpha/\lambda$. D_{fa}, D_o, D_i, D_s, and D_{ba} are the dynamic matrices in the form

$$D_\alpha = \begin{bmatrix} 1 & 1 \\ n_\alpha \cos\theta_\alpha & -n_\alpha \cos\theta_\alpha \end{bmatrix} \quad s \text{ wave}. \tag{10}$$

$$D_\alpha = \begin{bmatrix} \cos\theta_\alpha & \cos\theta_\alpha \\ n_\alpha & -n_\alpha \end{bmatrix} \quad p \text{ wave}. \tag{11}$$

θ_α and n_α ($\alpha = fa$, o, i, s, or ba) are the refracted angle and the refractive index of each medium. The reflection and transmission coefficients are defined as $r_s = B_{fa}^s/A_{fa}^s$ and $t_s = A_{ba}^s/A_{fa}^s$ for the s wave and $r_p = B_{fa}^p/A_{fa}^p$ and $t_p = A_{ba}^p/A_{fa}^p$ for the p wave. Finally, RDS and TDS signals are defined as

$$\frac{\Delta r}{r} = \frac{2(r_s - r_p)}{r_s + r_p}, \quad \frac{\Delta t}{t} = \frac{2(t_s - t_p)}{t_s + t_p}.$$

However, if more than one medium is anisotropic (homogeneous), the interface s and p waves are in general coupled to each other. They will propagate along different beam paths. According to Yeh.[14] the amplitudes of the incident, reflected, and transmitted beam can be obtained as

$$\begin{pmatrix} A_{fa}{}^{s} \\ B_{fa}{}^{s} \\ A_{fa}{}^{p} \\ B_{fa}{}^{p} \end{pmatrix} = D_{fa}{}^{-1} D_o P_o D_o{}^{-1} D_i P_i D_i{}^{-1} D_s P_s D_s{}^{-1} D_{ba} \times \begin{pmatrix} C_{ba}{}^{O} \\ E_{ba}{}^{O} \\ C_{ba}{}^{E} \\ E_{ba}{}^{E} \end{pmatrix}. \quad (12)$$

Note that the amplitudes $E_{ba}{}^{O}$ and $E_{ba}{}^{E}$ equal 0 because there is no reflected beam traveling backward into the substrate. The reflection–transmission coefficients and the RDS–TDS signals have the same definitions as in the isotropic layered structure. The elements of the 4×4 propagation and dynamic matrices depend on the dielectric tensor of the anisotropic layer and in general are difficult to obtain. However, we show that, at some specific orientations, the 4×4 matrices can be reduced to simple forms.

Consider the case when the principal dielectric axis of the interface z' is parallel to the laboratory z axis but the principal dielectric axes x' and y' are at an angle ϕ to the laboratory x and y axes, because we can rotate the sample along the xy plane. The dielectric tensor of the anisotropic layer becomes

$$\begin{bmatrix} \varepsilon_x \cos^2 \phi + \varepsilon_y \sin^2 \phi & \cos \phi \sin \phi(\varepsilon_x - \varepsilon_y) & 0 \\ \cos \phi \sin \phi(\varepsilon_x - \varepsilon_y) & \varepsilon_y \cos^2 \phi + \varepsilon_x \sin^2 \phi & 0 \\ 0 & 0 & \varepsilon_z \end{bmatrix}. \quad (13)$$

Note that when $\phi = 0°, 90°, 180°, 270°$ the dielectric tensor reduces to even simpler forms. We find that under these special rotational angles the s and p waves are decoupled. Therefore we can use the 2×2 matrix multiplication to calculate their reflectances separately. If $\theta_a > 0°$, the dynamic matrices of the interface i are

$$D_i = \begin{bmatrix} 1 & 1 \\ n_s \cos \theta_s & -n_s \cos \theta_s \end{bmatrix} \quad s \text{ wave}, \quad (14)$$

$$D_i = \begin{bmatrix} \cos \theta_p & \cos \theta_p \\ n_p & -n_p \end{bmatrix} \quad p \text{ wave}, \quad (15)$$

and the propagation matrices are

$$P_i = \begin{bmatrix} \exp(i2\pi n_s \cos \theta_s d_i/\lambda) & 0 \\ 0 & \exp(-i2\pi n_s \cos \theta_s d_i/\lambda) \end{bmatrix} \quad s \text{ wave}, \quad (16)$$

$$P_i = \begin{bmatrix} \exp(i2\pi n_p \cos \theta_p d_i/\lambda) & 0 \\ 0 & \exp(-i2\pi n_p \cos \theta_p d_i/\lambda) \end{bmatrix} \quad p \text{ wave}. \quad (17)$$

The refractive indexes n_s and n_p in Eqs. (14)–(17) depend on the angle ϕ. When $\phi = 0°$ or $180°$,

$$n_s = n_i{}^{x},$$

$$n_p = \left\{ (n_i{}^{y})^2 - (n_o)^2 \sin^2 \theta_o \left[\left(\frac{n_i{}^{y}}{n_i{}^{z}} \right)^2 - 1 \right] \right\}^{1/2}; \quad (18)$$

when $\phi = 90°$ or $270°$,

$$n_s = n_i{}^{x},$$

$$n_p = \left\{ (n_i{}^{x})^2 - (n_o)^2 \sin^2 \theta_o \left[\left(\frac{n_i{}^{x}}{n_i{}^{z}} \right)^2 - 1 \right] \right\}^{1/2}, \quad (19)$$

where the refractive indexes of the interface are $n_i{}^{x} = \sqrt{\varepsilon_x}$, $n_i{}^{y} = \sqrt{\varepsilon_y}$, and $n_i{}^{z} = \sqrt{\varepsilon_z}$.

For nonzero θ_a we see that the electric field vector $\mathbf{E}$ of any incident polarized light can be separated into two components, one parallel to the z axis and the other parallel to the xy plane, i.e.,

$$\mathbf{E} = A_s \mathbf{s} + A_p \mathbf{p} = A_s \mathbf{y} + A_p \cos \theta_a \mathbf{x} - A_p \sin \theta_a \mathbf{z}. \quad (20)$$

When $\tan \phi$ or $\tan(\phi \pm 180°)$ equals $A_s/(A_p \cos \theta_a) = 1/\cos \theta_a$ (45° polarized light beam, i.e., $A_s = A_p$), $\mathbf{E}_{xy} \| x'$ and the light beam will probe only one of the in-plane principal dielectric constant, ε_x. We also see that when $\tan(\phi \pm 90°)$, $\tan(\phi \pm 270°) = A_s/(A_p \cos \theta_a) = 1/\cos \theta_a$, $E_{xy} \| y'$ and the light beam will probe only the in-plane dielectric constant, ε_y. The RDS or TDS signal is produced only by the out-of-plane anisotropy ($\varepsilon_x \neq \varepsilon_z$ or $\varepsilon_y \neq \varepsilon_z$) of the interface.

Therefore, when $\phi = \tan^{-1}(1/\cos \theta_a)$ or $\phi = \tan^{-1}(1/\cos \theta_a) \pm 180°$,

$$n_s = n_i{}^{x},$$

$$n_p = \left\{ (n_i{}^{x})^2 - (n_o)^2 \sin^2 \theta_o \left[\left(\frac{n_i{}^{x}}{n_i{}^{z}} \right)^2 - 1 \right] \right\}^{1/2}. \quad (21)$$

When $\phi = \tan^{-1}(1/\cos \theta_a) \pm 90°$ or $\phi = \tan^{-1}(1/\cos \theta_a) \pm 270°$,

$$n_s = n_i{}^{y},$$

$$n_p = \left\{ (n_i{}^{y})^2 - (n_o)^2 \sin^2 \theta_o \left[\left(\frac{n_i{}^{y}}{n_i{}^{z}} \right)^2 - 1 \right] \right\}^{1/2}. \quad (22)$$

The dynamic matrices D_{fa}, D_o, D_s, and D_{ba} and the propagation matrices P_o and P_s remain the same as in the isotropic case.

The matrix method described above is an exact approach to the propagation of electromagnetic radiation in anisotropic layered media. Both birefringent phase retardation and thin-film interference are considered. The

general explicit forms of the reflection coefficients r_s, r_p, t_s, and t_p are too complicated to derive and are normally not available.

Numerical methods are used to generate the RDS and TDS spectra. We demonstrate the numerical method by considering an anisotropic interface sandwiched between two isotropic layers, a ZnSe overlayer and a GaAs substrate.

3. NUMERICAL ANALYSIS

The refractive indices of ZnSe and GaAs at different wavelengths were obtained from the literature.[17,18] Both of them are isotropic media. We have to generate the refractive index of the interface. We can assume that the interface is a modified ZnSe layer. We add three Lorentzian resonances to the principal refractive indices of ZnSe:

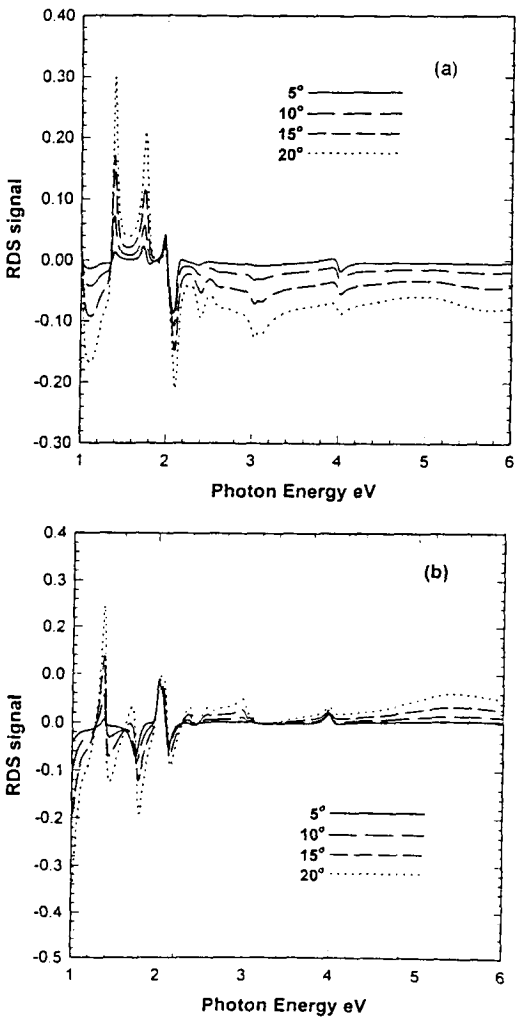

Fig. 1. (a) Real part and (b) imaginary part of the numerical RDS spectra generated at $\phi = 0°$ and different incident angles θ_a.

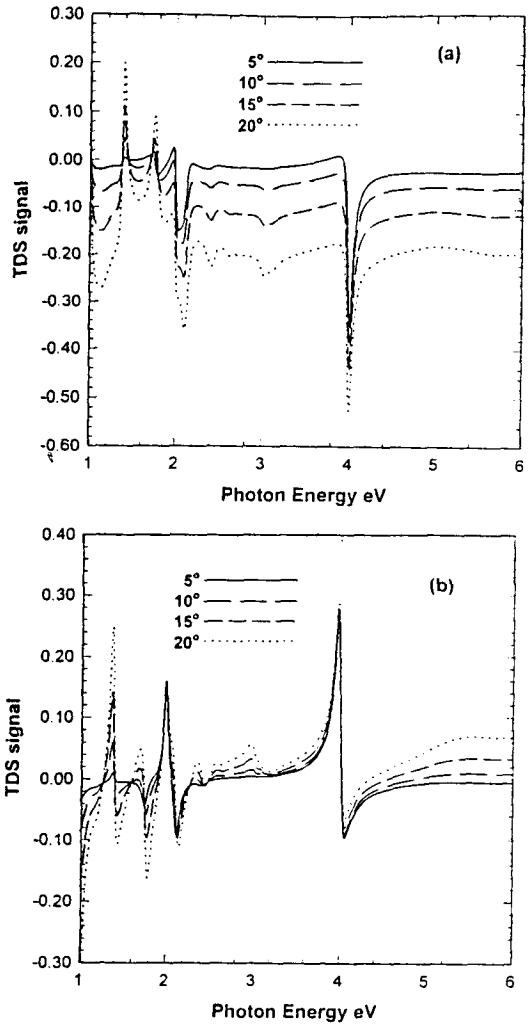

Fig. 2. (a) Real part and (b) imaginary part of the numerical TDS spectra generated at $\phi = 0°$ and different incident angles θ_a.

$$n_i^x = (\varepsilon_{\mathrm{ZnSe}} + \varepsilon_1 + \varepsilon_2 + \varepsilon_3)^{1/2},$$

$$n_i^y = (\varepsilon_{\mathrm{ZnSe}} + \varepsilon_2)^{1/2}, \quad n_i^z = (\varepsilon_{\mathrm{ZnSe}})^{1/2},$$

where

$$\varepsilon_1 = \frac{A_1}{E_1 - \hbar\omega - i\Gamma_1},$$

$$\varepsilon_2 = \frac{A_2}{E_2 - \hbar\omega - i\Gamma_2},$$

$$\varepsilon_3 = \frac{A_3}{E_3 - \hbar\omega - i\Gamma_3}$$

with the following parameters

$E_1 = 2.0$ eV, $E_2 = 3.00$ eV, $E_3 = 4.00$ eV;

$\Gamma_1 = 0.03$, $\Gamma_2 = 0.06$, $\Gamma_3 = 0.03$,

$A_1 = 0.4$, $A_2 = 6.0$, $A_3 = 0.8$.

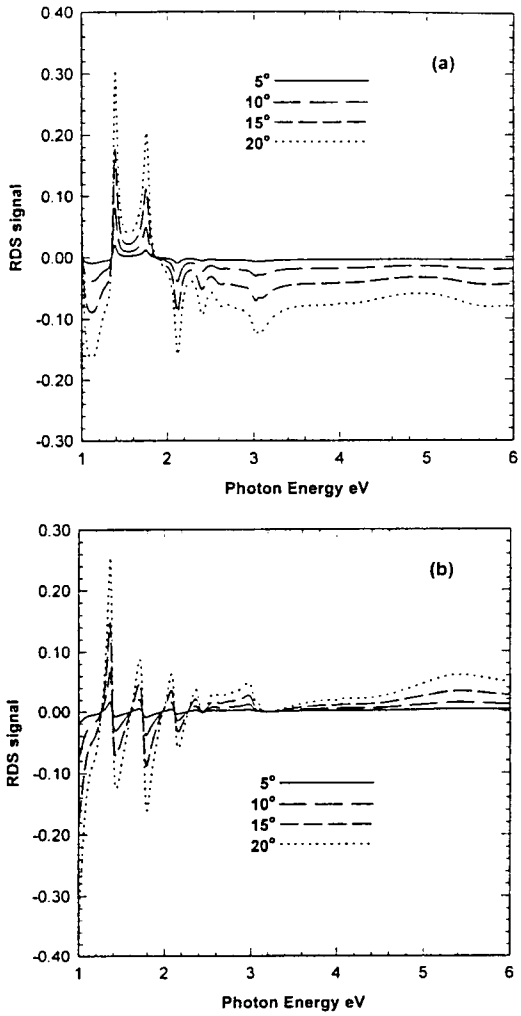

Fig. 3. (a) Real part and (b) imaginary part of the numerical RDS spectra generated at $\phi = \tan^{-1}(1/\cos\theta_a)$ and different incident angles θ_a.

We see that the in-plane anisotropy is induced by ε_1 and ε_3, whereas the out-of-plane anisotropy is induced by ε_2. Thicknesses of the ZnSe overlayer d_o of 100 nm, the interface d_i of 5 nm, and the GaAs substrate d_s of 300 nm were used in the calculation. We now show numerically that a RDS or a TDS spectrum can be separated into two parts, i.e., an in-plane biaxial spectrum and an out-of-plane uniaxial spectrum. The real and the imaginary parts of the RDS and TDS spectra generated at $\phi = 0°$ with different incident angles $\theta_a = 5°, 10°, 15°, 20°$ are depicted in Figs. 1 and 2. At this ϕ angle the in-plane anisotropy is maximum in the RDS and TDS spectra, so that both biaxial and uniaxial anisotropy contribute to the RDS and TDS signals. In Figs. 3 and 4 the RDS and TDS spectra are generated by the same parameters as in Figs. 1 and 2, except that $\phi = \tan^{-1}(1/\cos\theta_a)$. At this ϕ angle, the biaxial anisotropy no longer contributes to the RDS and TDS signals. We see that the out-of-plane anisotropy RD and TD signals become more significant as the incident angle increases. Now, if we subtract from the spectra of Figs. 1 and 2 the spectra shown in Figs. 3 and 4, we find that the resultant spectra are identical to the spectra generated at $\phi = 0°$ and $\theta_a = 0°$ (normal incidence), as shown in Figs. 5 and 6. When $\phi = 0°$ and $\theta_a = 0°$ the uniaxial anisotropies no longer contribute to the RDS and TDS signals. The excellent overlap of the spectra of Figs. 5 and 6 shows that the following relationships are true for $\theta_a \leq 20°$:

$$\frac{\Delta r}{r}\left(\begin{matrix}\phi = 0° \\ \theta_a \leq 20°\end{matrix}\right) = \frac{\Delta r}{r}\left(\begin{matrix}\phi = 0° \\ \theta_a = 0°\end{matrix}\right) + \frac{\Delta r}{r}\left[\begin{matrix}\phi = \tan^{-1}(1/\cos\theta_a) \\ \theta_a \leq 20°\end{matrix}\right], \tag{23}$$

$$\frac{\Delta t}{t}\left(\begin{matrix}\phi = 0° \\ \theta_a \leq 20°\end{matrix}\right) = \frac{\Delta t}{t}\left(\begin{matrix}\phi = 0° \\ \theta_a = 0°\end{matrix}\right) + \frac{\Delta t}{t}\left[\begin{matrix}\phi = \tan^{-1}(1/\cos\theta_a) \\ \theta_a \leq 20°\end{matrix}\right]. \tag{24}$$

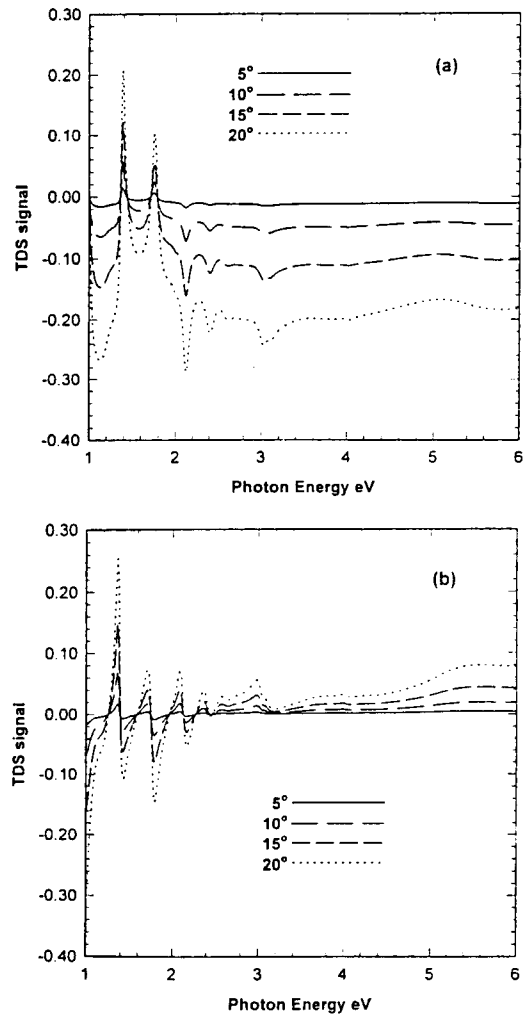

Fig. 4. (a) Real part and (b) imaginary part of the numerical TDS spectra generated at $\phi = \tan^{-1}(1/\cos\theta_a)$ and different incident angles θ_a.

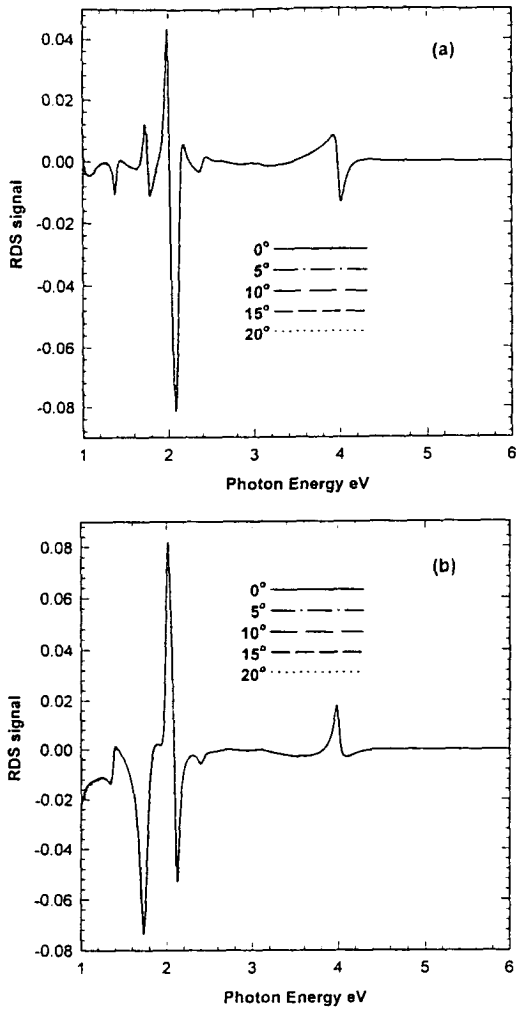

Fig. 5. (a) Real part and (b) imaginary part of the numerical RDS spectra of Fig. 1 after the spectra of Fig. 3 are subtracted; the spectrum is generated at $\phi = 0°$ and $\theta_a = 0°$.

Moreover, we find that

$$\frac{\Delta r}{r}\left(\begin{matrix}\phi = 90° \\ \theta_a \leqslant 20°\end{matrix}\right) = \frac{\Delta r}{r}\left(\begin{matrix}\phi = 90° \\ \theta_a = 0°\end{matrix}\right) + \frac{\Delta r}{r}\left[\begin{matrix}\phi = \tan^{-1}(1/\cos\theta_a) \pm 90° \\ \theta_a \leqslant 20°\end{matrix}\right], \tag{25}$$

$$\frac{\Delta t}{t}\left(\begin{matrix}\phi = 90° \\ \theta_a \leqslant 20°\end{matrix}\right) = \frac{\Delta t}{t}\left(\begin{matrix}\phi = 90° \\ \theta_a = 0°\end{matrix}\right) + \frac{\Delta t}{t}\left(\begin{matrix}\phi = \tan^{-1}(1/\cos\theta_a) \pm 90° \\ \theta_a \leqslant 20°\end{matrix}\right). \tag{26}$$

In other words, a RDS or a TDS spectrum acquired at $\phi = 0°$ or $\phi = 90°$ and $\theta_a \leqslant 20°$ can be separated into two parts, a biaxial spectrum induced by the in-plane anisotropy ($\varepsilon_x \neq \varepsilon_y$) and a uniaxial spectrum induced by the out-of-plane anisotropy ($\varepsilon_x \neq \varepsilon_z$ or $\varepsilon_y \neq \varepsilon_z$). We can simply interpret the upper boundary of θ_a at 20° by Eq. (20). From Eq. (20), E_{xy} will be parallel to x' if $\tan\phi = 1/\cos\theta_a$. When $\theta_a = 0°$ (normal incidence), $\phi = 45°$. As $\theta_a > 0°$, ϕ becomes larger than 45°. When $\theta_a = 20°$, $\Delta\phi = \phi - 45° = 1.781°$; when $\theta_a = 25°$, $\Delta\phi = 2.814°$. It seems that, provided that $\sin(\Delta\phi) \approx \Delta\phi$, a RDS or a TDS spectrum can be separated into two parts, a biaxial spectrum and a uniaxial spectrum.

4. CONCLUSION

In most published RDS studies normal-incidence reflection and thin anisotropic interface were assumed, although most of the RDS spectra were measured at nearly normal but, strictly speaking, nonnormal incidence. We have shown that a nonnormal incidence, even at 5°, will bring the off-plane anisotropy and the Fresnel reflectance–transmittance components of a surface–interface into the resultant RDS–TDS spectrum. Ignor-

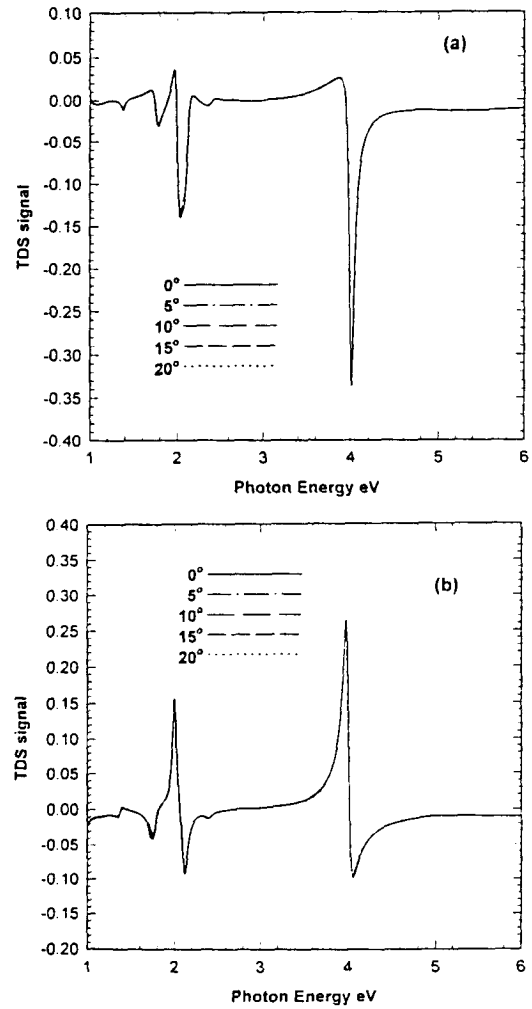

Fig. 6. (a) Real part and (b) imaginary part of the numerical TDS spectra of Fig. 2 after the spectra of Fig. 4 are subtracted; the spectrum is generated at $\phi = 0°$ and $\theta_a = 0°$.

ing their existence will result in great misinterpretation, for example, in our case, counting the out-of-plane anisotropy induced by ε_2 as the third in-plane anisotropy oscillation.

The Bereman formulism can completely generate nonnormal RDS–TDS spectra with finite layer thicknesses following the idea of Schubert.[18] However, by using either Yeh's or Berreman's formalism one cannot avoid complicated matrix multiplication. Definitely, a single-line equation will not simulate an accurate RDS–TDS spectrum of a multilayered system. Numerical analysis is the only practical way to acquire the dielectric constants of multilayered systems from RDS–TDS spectra.

We have extended the developed numerical method[15] to take into account the effects of nonnormal incidence on the RDS–TDS spectra of multilayer biaxial anisotropic systems with finite layer thicknesses. More-complicated systems can be systematically studied by our method. We have shown that when the principal dielectric axes of the interface are at certain orientations, the RDS–TDS spectra can be separated into two parts, a biaxial spectrum that depends on the in-plane anisotropy ($\varepsilon_x \neq \varepsilon_y$) and a uniaxial spectrum that depends on the out-of-plane anisotropy ($\varepsilon_x \neq \varepsilon_z$, $\varepsilon_y \neq \varepsilon_z$). We have further shown that the separation is valid for large in-plane anisotropy, i.e., when $|\varepsilon_x - \varepsilon_y|$ is comparable with $|\varepsilon_x|$ and the incident angle θ_a is $\leq 20°$. By separating the RDS spectra into two parts, we can systematically study the in-plane anisotropy and the out-of-plane anisotropy of any layered structures.

REFERENCES

1. D. E. Aspnes and A. A. Studna, Phys. Rev. Lett. **54**, 1956 (1985).
2. D. E. Aspnes, J. Vac. Sci. Technol. B **3**, 1498 (1985).
3. D. E. Aspnes, J. P. Harbison, A. A. Studna, and L. T. Florez, J. Vac. Sci. Technol. A **6**, 1327 (1988).
4. Z. Yang, G. W. Wong, I. K. Sou, and Y. H. Yeung, Appl. Phys. Lett. **66**, 2235 (1995).
5. H. Akinaya and K. Tanaka, Appl. Surf. Sci. **82/83**, 298 (1994).
6. T. Yasuda, D. E. Aspnes, D. R. Lee, C. H. Bjorkman, and G. Lucovsky, J. Vac. Sci. Technol. A **12**, 1152 (1994).
7. D. E. Aspnes, Mater. Sci. Eng. B **30**, 109 (1995).
8. I. Kamiya, D. E. Aspnes, L. T. Florez, and J. P. Harbison, Phys. Rev. B **46**, 15.894 (1992).
9. O. Acher, F. Omnes, and M. Razeghi, Mater. Sci. Eng. B **5**, 223 (1990).
10. J. S. Luo, J. M. Olson, S. R. Kurtz, D. J. Arent, and K. A. Bertness, Phys. Rev. B **51**, 7603 (1995).
11. K. Hingerl, D. E. Aspnes, I. Kamiya, and L. T. Florez, Appl. Phys. Lett. **63**, 885 (1993).
12. K. Hingerl, D. E. Aspnes, and I. Kamiya, Surf. Sci. **287/288**, 686 (1993).
13. S.-H. Wei and A. Zunger, Phys. Rev. B **51**, 14,110 (1995).
14. P. Yeh, *Optical Waves in Layered Media* (Wiley, New York, 1988).
15. T.-K. Kwok and Z. Yang, J. Appl. Phys. **80**, 4621 (1996).
16. D. E. Aspnes and A. A. Studna, Phys. Rev. B **27**, 985 (1983).
17. S. Adachi and T. Taguchi, Phys. Rev. B **43**, 9569 (1991).
18. M. Schubert, Phys. Rev. B **53**, 4265 (1996).